

## Magnetic phase transitions in $\text{Pr}_{1-x}\text{Dy}_x\text{Mn}_2\text{Ge}_2$ and $\text{Ce}_{1-x}\text{Dy}_x\text{Mn}_2\text{Ge}_2$

This article has been downloaded from IOPscience. Please scroll down to see the full text article.

2003 J. Phys.: Condens. Matter 15 653

(<http://iopscience.iop.org/0953-8984/15/4/306>)

View [the table of contents for this issue](#), or go to the [journal homepage](#) for more

Download details:

IP Address: 171.66.16.119

The article was downloaded on 19/05/2010 at 06:30

Please note that [terms and conditions apply](#).

# Magnetic phase transitions in $\text{Pr}_{1-x}\text{Dy}_x\text{Mn}_2\text{Ge}_2$ and $\text{Ce}_{1-x}\text{Dy}_x\text{Mn}_2\text{Ge}_2$

Ayhan Elmali<sup>1,3</sup>, Ilker Dincer<sup>1</sup>, Yalcin Elerman<sup>1</sup>, Helmut Ehrenberg<sup>2</sup>  
and Hartmut Fuess<sup>2</sup>

<sup>1</sup> Department of Engineering Physics, Faculty of Engineering, Ankara University,  
06100 Besevler-Ankara, Turkey

<sup>2</sup> Institute for Materials Science, Darmstadt University of Technology, Petersenstrasse 23,  
D-64287 Darmstadt, Germany

E-mail: elmali@eng.ankara.edu.tr

Received 24 October 2002

Published 20 January 2003

Online at [stacks.iop.org/JPhysCM/15/653](http://stacks.iop.org/JPhysCM/15/653)

## Abstract

The magnetic properties of the compounds  $\text{Pr}_{1-x}\text{Dy}_x\text{Mn}_2\text{Ge}_2$  ( $0 \leq x \leq 1$ ) and  $\text{Ce}_{1-x}\text{Dy}_x\text{Mn}_2\text{Ge}_2$  ( $0 \leq x \leq 1$ ) were investigated by means of temperature-dependent DC magnetization measurements in low external magnetic fields. The substitution of Dy for Pr or Ce leads to a linear decrease in the lattice parameters. Below about 330 K, the interlayer magnetic coupling in the Mn sublattice is ferromagnetic for Pr-rich and Ce-rich compounds and antiferromagnetic for Dy-rich compounds. At low temperatures, the Dy sublattice also orders and reconfigures the ordering in the Mn sublattice. This leads to ferrimagnetic ordering for Dy-rich compounds.

## 1. Introduction

The intermetallic compounds  $\text{RMn}_2\text{X}_2$  ( $\text{R}$  = rare earth,  $\text{X}$  = Si or Ge) have attracted considerable interest in the last decade due to the different magnetic configurations obtained by gradually replacing the rare-earth element by another lanthanide or gradually replacing Mn by another transitional element. The well known tetragonal  $\text{RMn}_2\text{Ge}_2$  compounds have been investigated by means of neutron diffraction, Mössbauer experiments, and magnetization measurements [1, 2]. In these compounds, both R and Mn atoms possess magnetic moments. According to the results of these investigations, the intralayer Mn–Mn exchange interaction is the strongest, leading to a ferromagnetic (FM) coupling of the Mn moments along the  $c$ -axis. On the other hand, the interlayer Mn–Mn exchange is very sensitive to the lattice parameter  $a$ , leading to FM or antiferromagnetic (AF) ordering of the Mn sublattice depending on the specific R element and temperature. The compounds with light rare earths ( $\text{R}$  = La–Nd) exhibit parallel alignment of Mn moments along the  $c$ -axis below the Curie temperature  $T_C^{\text{inter}}$ ,

<sup>3</sup> Author to whom any correspondence should be addressed.

and an AF alignment in (001) planes also occurs with a Néel temperature  $T_N^{intra} > T_C^{inter}$ . The *in-plane* antiferromagnetism can be commensurate or incommensurate with the lattice periodicity. In the case of heavy rare-earth elements, there is only AF alignment of Mn moments along the *c*-axis with the Néel temperature  $T_N^{inter}$ . The nature of the magnetic couplings in these compounds within and between the Mn layers is closely related to the *in-plane* Mn–Mn spacing  $d_{Mn-Mn}^a$ . Roughly, if  $d_{Mn-Mn}^a > 2.87 \text{ \AA}$  ( $a > 4.06 \text{ \AA}$ ), the *intralayer in-plane* coupling is AF and the *interlayer* coupling is FM. When  $2.84 \text{ \AA} < d_{Mn-Mn}^a < 2.87 \text{ \AA}$  ( $4.02 \text{ \AA} < a < 4.06 \text{ \AA}$ ), the *intralayer in-plane* coupling is again AF, but the *interlayer* coupling is also AF. In the case where  $d_{Mn-Mn}^a < 2.84 \text{ \AA}$  ( $a < 4.02 \text{ \AA}$ ), there is effectively no *intralayer in-plane* spin component, and the *interlayer* coupling remains AF [3, 4].

DyMn<sub>2</sub>Ge<sub>2</sub> has completely different magnetic properties [5–7] and shows a magnetocaloric effect above 40 K [8]. There is a large magnetic anisotropy due to the electronic configuration of the Dy<sup>3+</sup> ion; from the magnetization measurements, it is suggested that the Dy–Mn and Mn–Mn exchange interactions compete with each other. Due to the strong dependence of the *interlayer* Mn–Mn exchange interaction on the lattice parameter *a*, one can vary the  $d_{Mn-Mn}^a$ -value in the neighbourhood of the critical value by alloying different elements with DyMn<sub>2</sub>Ge<sub>2</sub> and observe the destruction, stabilization, and variation of different types of FM and AF phases. It is, therefore, attractive to investigate the magnetic properties of R<sub>1-x</sub>Dy<sub>x</sub>Mn<sub>2</sub>Ge<sub>2</sub> systems, where R is a light rare-earth metal. This might lead to the transition from parallel to antiparallel spin alignment in adjacent Mn layers. In such a study, it is possible to gain information on both *intralayer* and *interlayer* magnetic properties of Mn planes. In order to make use of the intrinsic pinning effect in these systems [9, 10] to characterize the various magnetic transitions, we performed low-field  $M(T)$  measurements on Pr<sub>1-x</sub>Dy<sub>x</sub>Mn<sub>2</sub>Ge<sub>2</sub> and Ce<sub>1-x</sub>Dy<sub>x</sub>Mn<sub>2</sub>Ge<sub>2</sub>. According to whether the sample is cooled with or without a low external field from the high-temperature AF phase to below the Curie temperature, the *interlayer* FM components are ‘pinned’ into different configurations. It is then possible to identify the transitions from the field-cooled (FC) or zero-field-cooled (ZFC) data, or both, according to the magnitudes of the features present. We also combine the results of magnetization measurements and earlier neutron diffraction and Mössbauer studies to give an account on the competing magnetic interactions.

## 2. The end-members PrMn<sub>2</sub>Ge<sub>2</sub>, CeMn<sub>2</sub>Ge<sub>2</sub>, and DyMn<sub>2</sub>Ge<sub>2</sub>

Before proceeding to the results, we briefly review the spin structures in the various magnetic states of the end-members PrMn<sub>2</sub>Ge<sub>2</sub>, CeMn<sub>2</sub>Ge<sub>2</sub>, and DyMn<sub>2</sub>Ge<sub>2</sub>. In PrMn<sub>2</sub>Ge<sub>2</sub>, *intralayer in-plane* AF ordering occurs below the Néel temperature  $T_N^{intra} = 415 \text{ K}$  [11, 12]. Cooling to temperatures below the ‘Curie’ temperature  $T_C^{inter} \approx 330 \text{ K}$  leads to a canted spin structure with the *c*-axis *interlayer* spin components aligning parallel [12–17]. Below 280 K, the magnetic structure transforms from a canted to a conical configuration with a cone semiangle of approximately 58° [13]. The *c*-axis *interlayer* alignment remains parallel. The Pr sublattices are magnetically disordered at these high temperatures and order along the *c*-axis parallel to the Mn moments only below  $T_C^{Pr} \approx 100 \text{ K}$  [13].

CeMn<sub>2</sub>Ge<sub>2</sub> is a ferromagnet below the Curie temperature of 320 K [13, 18, 19]. In this compound, the Mn sublattice has a conical magnetic structure with the cone semiangle of approximately 56° while the Ce moments do not order at any temperature. The Mössbauer spectroscopy and neutron diffraction studies give evidence for a transition from ferromagnetism to antiferromagnetism at 320 K, and the compound is paramagnetic only above 410 K.

In  $\text{DyMn}_2\text{Ge}_2$  below 438 K, the Mn sublattice orders antiferromagnetically [5, 6]. According to the results of neutron diffraction experiments performed at  $T \leq 300$  K, the spins in each of the Mn layers align parallel along the  $c$ -axis, and spins in alternating Mn layers align in the up–down sequence of a collinear antiferromagnet. The Dy and Mn sublattices each acquire FM alignment along the  $c$ -axis below 34 K and are antiparallel to each other, resulting in a collinear ferrimagnet. In the small temperature interval between 36 and 40 K, an intermediate (IM) magnetic phase with an  $\uparrow\downarrow\uparrow\downarrow\uparrow$  spin ordering sequence of the Mn layers is observed.

### 3. Experimental details

Polycrystalline samples of  $\text{Pr}_{1-x}\text{Dy}_x\text{Mn}_2\text{Ge}_2$  with  $x = 0, 0.2, 0.4, 0.55, 0.6, 0.65, 0.7, 0.8,$  and 1.0 and  $\text{Ce}_{1-x}\text{Dy}_x\text{Mn}_2\text{Ge}_2$  with  $x = 0, 0.2, 0.4, 0.6, 0.65, 0.7, 0.75, 0.8,$  and 1.0 were synthesized by arc melting the elements on a water-cooled Cu hearth under purified argon gas. The purity of the elements was 99.9% for Pr, 99.9% for Ce, 99.9% for Dy, 99.98% for Mn, and 99.9999% for Ge. The mass loss of Mn during melting was compensated for by adding 2% excess Mn. The ingots were melted five times to attain homogeneity. X-ray analysis of the samples showed that any impurity was present at less than 3%. The samples were characterized by means of powder x-ray diffraction on a SIEMENS D-500 diffractometer using Cu  $K\alpha$  radiation and a secondary monochromator. The magnetization was measured using a SQUID magnetometer in the temperature range 5–350 K. The samples were first heated above  $T_C^{\text{inter}}$  and then measured in a ZFC–FC sequence.

### 4. Discussion of the results

#### 4.1. X-ray results for $\text{Pr}_{1-x}\text{Dy}_x\text{Mn}_2\text{Ge}_2$ and $\text{Ce}_{1-x}\text{Dy}_x\text{Mn}_2\text{Ge}_2$

Rietveld refinements based on the x-ray diffraction patterns, obtained at room temperature, confirmed the  $\text{ThCr}_2\text{Si}_2$ -type structure with space group  $I4/mmm$  for all samples of  $\text{Pr}_{1-x}\text{Dy}_x\text{Mn}_2\text{Ge}_2$  and  $\text{Ce}_{1-x}\text{Dy}_x\text{Mn}_2\text{Ge}_2$ . A trace of an impurity phase was also observed except for the samples with  $x = 0$  and 0.2. The refined tetragonal lattice parameters  $a$  and  $c$ , the unit-cell volume  $V$ , and the  $in$ -plane Mn–Mn spacing  $d_{\text{Mn–Mn}}^a$ , for both systems, are shown in figures 1 and 2. The substitution of Dy for Pr and Ce causes a linear decrease of the lattice parameters  $a$  and  $c$ , and the unit-cell volume  $V$ , obeying Vegard’s law for these pseudo-ternary compounds. The decrease of these parameters is a result of the smaller atomic radius of Dy compared with Pr and Ce. As a consequence, the decrease of the lattice parameters results in a decrease of the  $in$ -plane Mn–Mn spacing  $d_{\text{Mn–Mn}}^a$  and the  $inter$ layer nearest Mn–Mn distance.

#### 4.2. Magnetic properties of $\text{Pr}_{1-x}\text{Dy}_x\text{Mn}_2\text{Ge}_2$

The FC and ZFC magnetizations in a low external field of 5 mT are shown in figure 3. Results of magnetization measurements as a function of temperature show qualitatively different behaviours for different compositions. The type of magnetic ordering above  $T_N^{\text{intra}}$  has been clarified by neutron diffraction and Mössbauer studies on  $\text{PrMn}_2\text{Ge}_2$  [11, 12]. Below the Néel temperature 415 K, the ordering is found to be AF only in the Mn  $intra$ layer with moments in the (001) Mn planes. Below  $T_C^{\text{inter}}$ , the magnetization of  $\text{PrMn}_2\text{Ge}_2$  increases with decreasing temperature as expected for a system with FM coupling. The data for  $x = 0$  show a distinct feature at about 280 K in both the FC and ZFC states. This temperature corresponds to the temperature of the transition from the canted to the conical spin structure observed in neutron

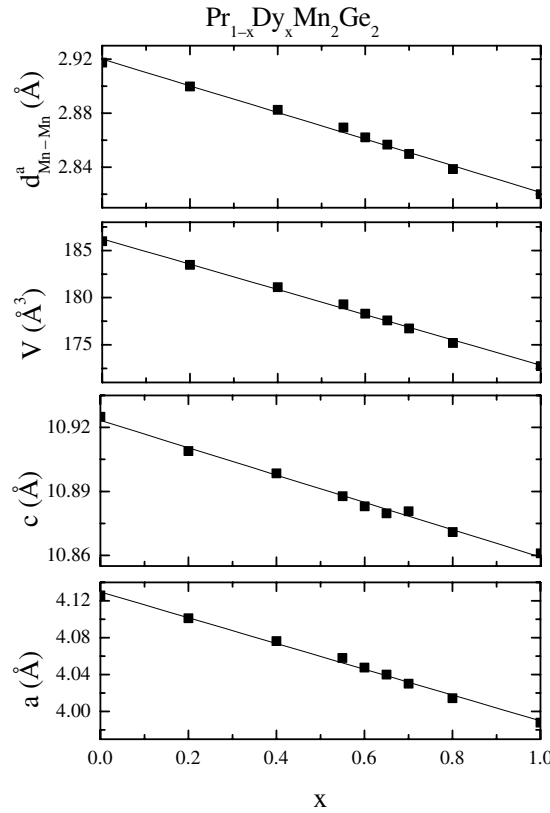


**Figure 1.** The concentration dependence of the *intralayer* Mn–Mn spacing  $d_{\text{Mn–Mn}}^a$ , the lattice constants  $c$  and  $a$ , and the atomic volume  $V$  for  $\text{Pr}_{1-x}\text{Dy}_x\text{Mn}_2\text{Ge}_2$ .

diffraction studies and is designated as  $T_{c/c}$  [12]. Increases at  $T_C^R = 100$  and 80 K in the FC curves for the compounds with  $x = 0$  and 0.2, respectively, are attributed to the onset of ordering for the Pr sublattice.

The temperature dependence of the magnetization of the  $x = 0.2$  sample shows a similar behaviour to that of  $\text{PrMn}_2\text{Ge}_2$ . However, the magnetizations of the samples with  $0.4 \leq x \leq 0.65$  increase with decreasing temperature and, at about 100 K, they begin to decrease down to  $T_C^R$ . The overall magnetization decreases with increasing Dy concentration due to a strengthening of the AF interaction in the Mn sublattice. Samples with  $0.55 \leq x \leq 0.65$  show an IM phase, as clearly seen for  $x = 0.65$  in figure 3. We consider the temperature at the maximum of magnetization as a reference point  $T_{IM}$  (see table 1) where the AF ordering sets in. At  $T_{IM} < T_C^{\text{inter}}$  the alloys enter an IM phase in which the canted ferromagnetism approaches an AF arrangement as the lattice contracts with decreasing temperature. This is a continuous transition that occurs in a composition range where the critical lattice spacing ( $d_{\text{Mn–Mn}}^a \approx 2.83\text{--}2.88$  Å) appears within the temperature range investigated, as found in the  $\text{Pr}_{1-x}\text{Y}_x\text{Mn}_2\text{Ge}_2$  [16]. For  $x = 0.65$ , the Néel temperature of the  $c$ -axis antiferromagnetism ( $T_N^{\text{inter}}$ ) was determined and is given in table 2. A small increase in the magnetizations of these samples with  $x = 0.55, 0.6, 0.65$  at about 80 K is related to the onset of ordering for the Pr and Dy sublattices. This increase in the magnetizations of  $\text{Ce}_{1-x}\text{Dy}_x\text{Mn}_2\text{Ge}_2$  is not observed, because Ce does not order. The rare-earth sublattice orders below  $T_C^R$ . The temperature  $T_C^R$  is obtained from the inflection point of the derivative of the magnetization. Below  $T_C^R$ , a FM

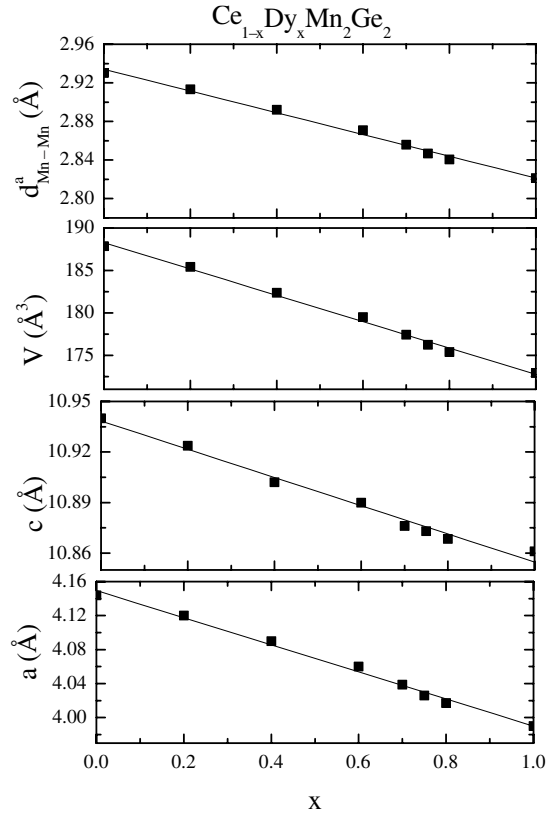


**Figure 2.** The concentration dependence of the *intralayer* Mn–Mn spacing  $d_{\text{Mn-Mn}}^a$ , the lattice constants  $c$  and  $a$ , and the atomic volume  $V$  for  $\text{Ce}_{1-x}\text{Dy}_x\text{Mn}_2\text{Ge}_2$ .

**Table 1.** The magnetic transition temperatures  $T_C^{\text{inter}}$ ,  $T_N^{\text{inter}}$ ,  $T_C^R$ ,  $T_N^{\text{inter-intra}}$ ,  $T_{IM}$ ,  $T_{c/c}$  for  $\text{Pr}_{1-x}\text{Dy}_x\text{Mn}_2\text{Ge}_2$ .

$x$ (nominal)	$T_C^{\text{inter}}$ (K)	$T_N^{\text{inter}}$ (K)	$T_C^R$ (K)	$T_N^{\text{inter-intra}}$ (K)	$T_{IM}$ (K)	$T_{c/c}$ (K)
0.0	330		100			280
0.2	338		80			
0.4	339		71			
0.55	340		64		255	
0.6	339		65		270	
0.65	335	205	59		285	
0.7			55	290		
0.8			53	305		
1.0			40	335		

phase is caused by the tendency of the Dy moments to align antiparallel to both the Pr and the Mn moments.

At around 300 K, magnetizations of the compounds with  $x = 0.7, 0.8,$  and  $1.0$  show an increase in the FC and the ZFC states with decreasing temperature, as clearly seen for  $x = 0.8$  and  $1.0$  in figure 4. This increase and the splitting between FC and ZFC curves indicate a weak FM component perpendicular to the  $c$ -axis due to a non-collinearity in the AF alignment.

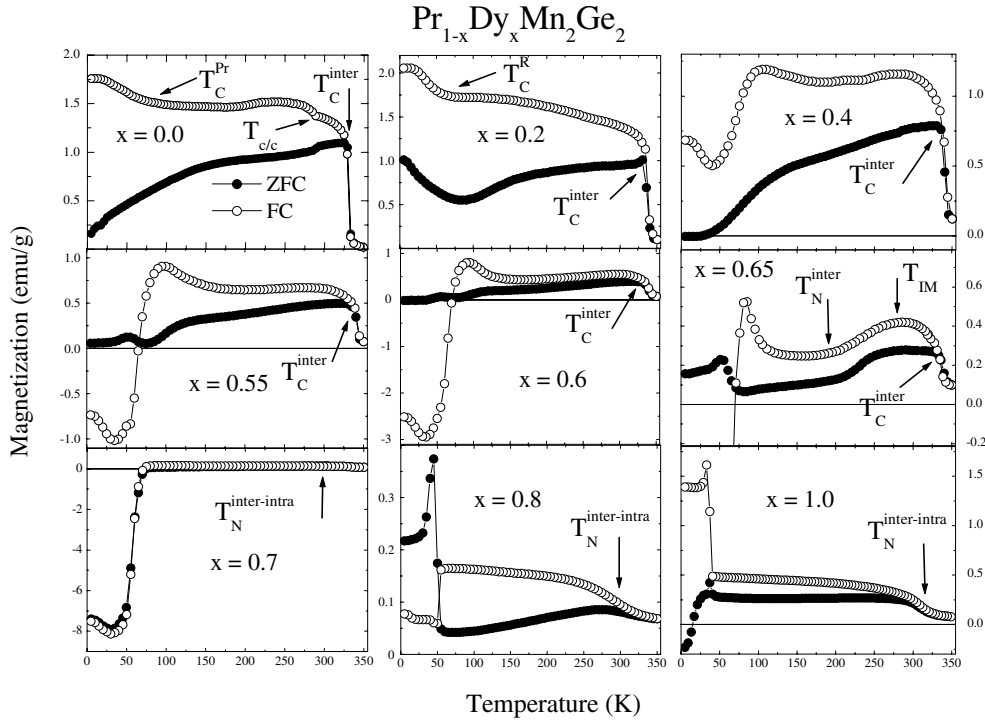


**Figure 3.** Temperature dependences of the FC and ZFC magnetizations of  $\text{Pr}_{1-x}\text{Dy}_x\text{Mn}_2\text{Ge}_2$  compounds in an applied field of 5 mT. The zoom for the  $x = 0.65$  compound is given to make the IM phase clear.

**Table 2.** The magnetic transition temperatures  $T_C^{\text{inter}}$ ,  $T_N^{\text{inter}}$ ,  $T_C^{\text{Dy}}$ ,  $T_N^{\text{inter-intra}}$ ,  $T_{IM}$ ,  $T_{c/c}$  for  $\text{Ce}_{1-x}\text{Dy}_x\text{Mn}_2\text{Ge}_2$ .

$x$ (nominal)	$T_C^{\text{inter}}$ (K)	$T_N^{\text{inter}}$ (K)	$T_C^{\text{Dy}}$ (K)	$T_N^{\text{inter-intra}}$ (K)	$T_{IM}$ (K)	$T_{c/c}$ (K)
0.0	320					284
0.2	328					
0.4	332		68			
0.6	338		62		270	
0.65	337		55			
0.7	334	190	53		280	
0.75			52	280		
0.8			50	300		
1.0			40	335		

These transition temperatures  $T_N^{\text{inter-intra}}$ , for the transition from (001) plane to  $c$ -axis AF ordering, are also listed in table 1. A similar effect is also observed in  $\text{Pr}_x\text{Tb}_{1-x}\text{Mn}_2\text{Ge}_2$  [10],  $\text{Ce}_x\text{Gd}_{1-x}\text{Mn}_2\text{Ge}_2$  [20], and  $\text{Nd}_{1-x}\text{Dy}_x\text{Ge}_2\text{Mn}_2$  [21]. The compounds with  $x = 0.7, 0.8,$  and  $1.0$  exhibit ' $c$ -axis antiferromagnetism' below  $T_N^{\text{inter-intra}}$  down to  $T_C^R$ . Below  $T_C^R$ , however, the average moment of the Dy-rich rare-earth sublattice is now aligned antiparallel to the Mn moment and the Pr moment and leads, to a good approximation, to ferrimagnetic order, as observed in neutron diffraction experiments for  $x = 1.0$  [5, 6]. In this case the overall magnetization increases with increasing Dy concentration because of the dominant magnetic moment of Dy.

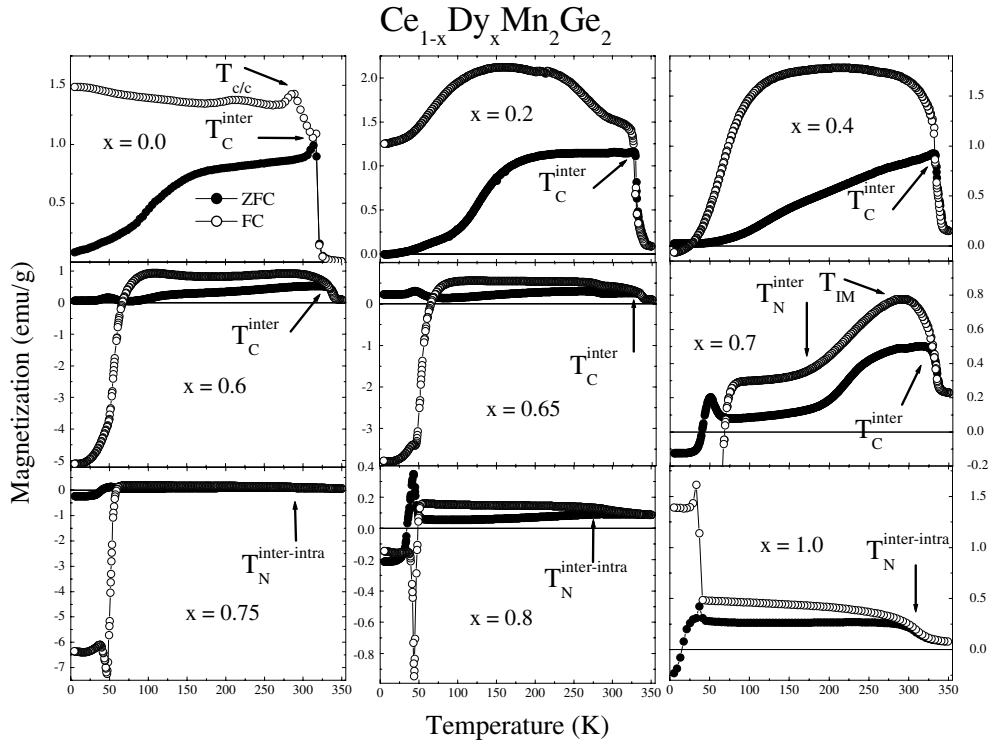


**Figure 4.** Temperature dependences of the FC and ZFC magnetizations of  $\text{Ce}_{1-x}\text{Dy}_x\text{Mn}_2\text{Ge}_2$  compounds in an applied field of 5 mT. The zoom for the  $x = 0.7$  compound is given to make the IM phase clear.

Large differences between the FC and ZFC modes indicate a different configurational pinning for each mode of measurement. The *interlayer* FM component is pinned by the anisotropy of the *intra*layer AF component of the Mn sublattice when the system is cooled through  $T_C^{\text{inter}}$  with or without an applied field [9, 10]. Just below  $T_C^{\text{inter}}$ , a strong splitting is found for the samples with  $x \leq 0.65$ . Cooling from the AF state at  $T_C^{\text{inter}} < T < T_N^{\text{intra}}$  and through  $T_C^{\text{inter}}$  in an external magnetic field gives a preferred orientation of the FM components. In the ZFC case, a preferred orientation is not induced, and, therefore, the total magnetization is weaker than in the FC case. In both cases, the *interlayer* FM components are pinned by the higher anisotropy of the *intra*layer AF component. Such a pinning effect is not observed for  $x \geq 0.7$ . For  $x = 0.65$ , the *interlayer* ‘FM’ coupling is very weak, and for  $x \geq 0.7$  there is no *interlayer* ‘FM’ coupling. By exploring this effect,  $T_C^{\text{inter}}$  can be determined with good precision from the 5 mT data. The splitting of the FC and ZFC curves for  $x = 0$  occurs at 330 K, which corresponds to  $T_C^{\text{inter}}$  found by neutron diffraction studies [12, 13]. Therefore,  $T_C^{\text{inter}}$  for the other samples is also determined from similar features in their magnetization curves.

#### 4.3. Magnetic properties of $\text{Ce}_{1-x}\text{Dy}_x\text{Mn}_2\text{Ge}_2$

The FC and ZFC magnetizations in a low external field of 5 mT are shown in figure 4.  $\text{CeMn}_2\text{Ge}_2$  is a ferromagnet below  $T_C^{\text{inter}} = 320$  K. For all compounds with  $x \leq 0.4$ , magnetizations increase rapidly at  $T_C^{\text{inter}} \approx 320$  K, at which a FM alignment of the Mn



moments has been found in neutron diffraction experiments for  $x = 0.0$  [13, 19]. Therefore, this temperature, obtained from the inflection point of the derivative of the magnetization, can be assigned to the Curie temperature of FM alignment of Mn sublattices for  $x = 0.0$ , and the same criterion can be applied for the other compounds with  $x > 0.0$ . This procedure provides Curie temperatures consistent with the analysis of the pinning effect. With decreasing temperature below the Curie point, there is a small maximum in the magnetization of the compound with  $x = 0.0$  at about 284 K. This temperature  $T_{c/c}$  may correspond to the temperature of the transition from the canted to the conical spin structure as observed in  $\text{Pr}_{1-x}\text{Dy}_x\text{Mn}_2\text{Ge}_2$ . However, at low temperatures, the magnetizations of the  $x = 0.2$  and  $0.4$  compounds show a progressive decrease with decreasing temperature. The overall magnetizations of the samples decrease with increasing  $x$ ; this is related to the substitution of Dy for Ce which introduces more pronounced AF interactions between two Mn layers. An IM state similar to that in  $\text{Pr}_{1-x}\text{Dy}_x\text{Mn}_2\text{Ge}_2$  is also observed for  $\text{Ce}_{1-x}\text{Dy}_x\text{Mn}_2\text{Ge}_2$ : samples with  $0.6 \leq x \leq 0.7$  show IM phases, as clearly seen in figure 4 for  $x = 0.7$ .  $T_{IM}$  cannot be determined for the  $x = 0.65$  compound. At  $T_{IM} < T_C^{inter}$  the ferromagnetism progresses towards antiferromagnetism as the lattice parameters change on decreasing the temperature. Below the IM state, when the lattice parameters become sufficiently small, an AF state becomes stable. For  $x = 0.7$ , the Néel temperature of the  $c$ -axis antiferromagnetism ( $T_N^{inter}$ ) was determined and this is given in table 2. The rare-earth sublattice orders below  $T_C^{Dy}$ . The temperature  $T_C^{Dy}$  is obtained from the inflection point of the derivative of the magnetization. Below  $T_C^{Dy}$ , the average moment of the Dy-rich rare-earth sublattice is aligned antiparallel to the Mn moments, and the system enters a ferrimagnetic phase.

At about 300 K, the anomalies in the magnetizations of  $\text{Pr}_{1-x}\text{Dy}_x\text{Mn}_2\text{Ge}_2$  are also observed for  $\text{Ce}_{1-x}\text{Dy}_x\text{Mn}_2\text{Ge}_2$ . For the compounds with  $x = 0.75, 0.8$ , and  $1.0$ , an increase in the FC and the ZFC states with decreasing temperature (clearly seen for  $x = 0.8$  and  $1.0$  in figure 4) is associated with a transition from  $ab$ -plane to  $c$ -axis AF ordering. This increase, along with the splitting, may also suggest a weak FM component in a direction other than that of the  $c$ -axis. The compounds with  $x = 0.75, 0.8$ , and  $1.0$  exhibit  $c$ -axis antiferromagnetism below  $T_N^{inter-intra}$  persisting down to  $T_C^{Dy}$ . The transition temperatures  $T_N^{inter-intra}$  are listed in table 2. Below  $T_C^{Dy}$ , the Dy sublattice orders, as seen from the rapid increase with decreasing temperature. This leads also to an interlayer FM component for the Mn sublattice. The average moment of the Dy-rich rare-earth sublattice is aligned antiparallel to the Mn moment and the system goes to a ferrimagnetic phase.  $\text{Pr}_{1-x}\text{Dy}_x\text{Mn}_2\text{Ge}_2$  and  $\text{Ce}_{1-x}\text{Dy}_x\text{Mn}_2\text{Ge}_2$  show similar ferrimagnetic ordering, although Ce does not order. The magnetic moment of the Dy sublattice decreases with increasing Ce content, and the total magnetic moment of the Mn sublattice can be compensated for by the magnetic moment of the Dy sublattice at lower temperature.

A pinning effect is also observed in  $\text{Ce}_{1-x}\text{Dy}_x\text{Mn}_2\text{Ge}_2$  similar to that in  $\text{Pr}_{1-x}\text{Dy}_x\text{Mn}_2\text{Ge}_2$ : a pronounced splitting between the ZFC and FC curves indicates that the *interlayer* FM component of the Mn moments is pinned by the anisotropy of the *in-plane* antiferromagnetism. By cooling from an AF state through  $T_C^{inter}$  in an external field, preferred orientation of the FM components is induced. In the ZFC case, the FM components of the Mn moments are pinned randomly and, therefore, the overall magnetization of the sample is smaller in the ZFC case than in the FC case.

## 5. Conclusions

Both  $\text{Pr}_{1-x}\text{Dy}_x\text{Mn}_2\text{Ge}_2$  and  $\text{Ce}_{1-x}\text{Dy}_x\text{Mn}_2\text{Ge}_2$  are ferromagnets below about 330 K ( $T_C^{inter}$ ), and FM Mn planes are ordered parallel along the  $c$ -axis for the Pr-rich and Ce-rich compounds.

For both systems, the overall magnetization decreases with increasing Dy concentration and FM Mn planes begin to align antiparallel along the  $c$ -axis. Increasing replacement of Pr by Dy or Ce by Dy causes a depression of FM ordering and the gradual development of AF ordering. This FM  $\rightarrow$  AF phase transition leads to an IM phase. The appearance of this IM phase is related to the thermal contraction of the lattice parameter  $a$ . Below  $T_C^R$ , the Dy magnetic moments of Dy-rich compounds begin to order, and the tendency of the Dy moments to align antiparallel to the Pr and Mn moments in  $\text{Pr}_{1-x}\text{Dy}_x\text{Mn}_2\text{Ge}_2$  and only the Mn moments in  $\text{Ce}_{1-x}\text{Dy}_x\text{Mn}_2\text{Ge}_2$ , and this leads to ferrimagnetic ordering.

For both systems, a large splitting between the ZFC and FC curves is observed at  $T_C^{\text{inter}}$ . This indicates that the FM component of the Mn moments is pinned by the anisotropy of the  $in$ -plane antiferromagnetism. On the basis of the pinning effect,  $T_C^{\text{inter}}$  can be determined with good precision from magnetization data obtained in low external fields.

### Acknowledgments

AE and YE thank the Alexander von Humboldt Foundation for support. This work was further supported by the University of Ankara Research Funds (Grant Number 20010705044) and TÜBITAK-BMBF Bilateral Programme (Grant Numbers MISAG-JÜLICH-1 and WTZ 42.6.BOA.6.A, respectively.)

### References

- [1] Szytula A and Leciejewicz J 1989 *Handbook on the Physics and Chemistry of Rare Earths* vol 12, ed K A Gschneidner Jr and L Eyring (Amsterdam: Elsevier) p 133
- [2] Szytula A and Buschow K H J (ed) 1991 *Handbook of Magnetic Materials* vol 6 (Amsterdam: Elsevier) p 85
- [3] Venturini G, Welter R, Ressouche E and Malaman B 1995 *J. Magn. Magn. Mater.* **150** 197
- [4] Venturini G, Malaman B and Ressouche E 1996 *J. Alloys Compounds* **240** 139
- [5] Kobayashi H, Onodera H, Yamaguchi Y and Yamamoto H 1991 *Phys. Rev. B* **43** 728
- [6] Venturini G, Malaman B, Tomala K, Szytula A and Sanchez J P 1992 *Phys. Rev. B* **46** 207
- [7] Lagutin A S, Levitin R S, Vanacken J and Bruynseraede Y 2002 *J. Magn. Magn. Mater.* **241** 190
- [8] Wada H, Tanabe Y, Hagiwara K and Shiga M 2002 *J. Magn. Magn. Mater.* **218** 203
- [9] Nowik I, Felner I and Bauminger I R 1997 *Phys. Rev. B* **55** 3033
- [10] Duman E, Acet M, Elerman Y, Elmali A and Wassermann E F 2002 *J. Magn. Magn. Mater.* **238** 11
- [11] Nowik I, Levi Y, Felner I and Bauminger E R 1995 *J. Magn. Magn. Mater.* **147** 135
- [12] Venturini G 1996 *J. Alloys Compounds* **232** 133
- [13] Welter R, Venturini G, Ressouche E and Malaman B 1995 *J. Alloys Compounds* **218** 204
- [14] Narasimhan K S V L, Rao V U S, Berger R L and Wallace W E 1975 *J. Appl. Phys.* **46** 4957
- [15] Iwata N, Ikeda T, Shigeoka T, Fujii H and Okamoto T 1986 *J. Magn. Magn. Mater.* **54–57** 481
- [16] Wang Y, Yang F, Chen C, Tang N and Wang O 1997 *J. Phys.: Condens. Matter* **9** 8539
- [17] Szytula A and Szott I 1981 *Solid State Commun.* **40** 199
- [18] Nowik I, Levi Y, Felner I and Bauminger E R 1995 *J. Magn. Magn. Mater.* **147** 373
- [19] Fernandez-Baca J A, Hill P, Chakoumakos B C and Ali N 1996 *J. Appl. Phys.* **79** 8
- [20] Kevran S, Acet M and Elerman Y 2001 *Solid State Commun.* **119** 95
- [21] Elerman Y, Kevran S, Duman E and Acet M 2002 *J. Magn. Magn. Mater.* at press